

# Fabrication of polymer microcomponents using CO<sub>2</sub> laser melting technique<sup>\*)</sup>

Wen Sheng Tan<sup>1), 2), \*\*)</sup>, Jian Zhong Zhou<sup>1)</sup>, Shu Huang<sup>1)</sup>, Wei Li Zhu<sup>1)</sup>, Xian Kai Meng<sup>1)</sup>

DOI: dx.doi.org/10.14314/polimery.2015.192

**Abstract:** A new method of laser melting molding to produce high-efficiency and high-quality polymer microcomponents was proposed. Numerical simulation was used to analyze the temperature changes of polymer melt during the laser irradiation process. An orthogonal experiment was also employed to investigate the factors influencing molding accuracy. The molding experiments were conducted on molds with various degrees of roughness, and the surface quality of the molded pieces was tested. The simulation analysis and experimental results showed that the laser power plays a critical role in improving the repetition accuracy. The next factors are irradiation time and mold temperature, followed by molding force. Optimized technological parameters (1.2 W of laser power, 6 mm of laser beam width, 6 s irradiation time, 150 N molding force, and 80 °C mold temperature) were applied to obtain a molded pieces with high repetition accuracy and a microstructure dimensional deviation of less than 1 μm. Using a mold with lower surface roughness provides that we can obtain a molded piece with lower roughness, the roughness difference between the mold and the molded piece was less than 0.012 μm.

**Keywords:** molding, polymer microcomponents, CO<sub>2</sub> laser, irradiation, numerical simulation.

## Wytwarzanie mikroelementów polimerowych z zastosowaniem techniki topienia laserem CO<sub>2</sub>

**Streszczenie:** Zaproponowano nową metodę formowania mikroelementów polimerowych z zastosowaniem topienia laserowego, zapewniającą wysoką wydajność oraz dobrą jakość wytwarzanych mikroelementów. Istotnym parametrem procesu, wpływającym na jakość formowanych elementów, jest temperatura stopu polimeru. Do analizy zmian tej temperatury pod wpływem napromieniania laserem zastosowano symulację numeryczną. Zastosowano także ortogonalny plan eksperymentu w celu zbadania czynników wpływających na dokładność formowania. Formowania przeprowadzono z użyciem form o różnych stopniach chropowatości i zbadano jakość powierzchni mikroelementów. Analiza wyników symulacji i badań eksperymentalnych wykazała, że moc lasera odgrywa kluczową rolę w uzyskaniu powtarzalnej dokładności. Kolejnymi czynnikami są czas napromieniania i temperatura formy oraz siły formujące. Zoptymalizowane parametry technologiczne (moc lasera 1,2 W, szerokość wiązki lasera 6 mm, czas napromieniania 6 s, siła formująca 150 N i temperatura formowania 80 °C) zastosowano do formowania elementów z powtarzalną dużą dokładnością odtwarzania wymiarów (odchylenia wymiarów nie przekraczały 1 μm). Użycie form o mniejszej chropowatości powierzchni pozwalało także uzyskać mniejszą chropowatość mikroelementów, przy czym różnica chropowatości formy i otrzymanego elementu była mniejsza niż 0,012 μm.

**Słowa kluczowe:** formowanie, mikroelementy polimerowe, laser CO<sub>2</sub>, napromienianie, symulacja numeryczna.

<sup>1)</sup> Center for Photon Manufacturing Science and Technology, School of Mechanical Engineering, Jiangsu University, Zhenjiang 212013, People's Republic of China.

<sup>2)</sup> Changzhou College of Information Technology, Changzhou, Jiangsu 213164, People's Republic of China.

<sup>\*)</sup> Materials contained in this article were presented at Global Conference on Polymer and Composite Materials, 27–29 May 2014, Ningbo, China.

<sup>\*\*) Author for correspondence; e-mail: tws.163@163.com</sup>

Polymer microcomponent (PMC) typically refers to a high-accuracy plastic molded piece with mm-scale matrix with local structural characteristics of tens and hundreds of μm (e.g., microfluidic chip of polymer, light guide plate, micro gear, and cell culture dishes). Compared with microcomponents made of metal, silicon, and glass, PMC uses cheaper raw material. The physical and chemical properties of PMC are stable, and PMC is easy to mold. In fields such as electronics, precision instruments, life and pharmaceutical engineering, and others, PMC has economic and academic research significance

[1]. At present, PMC molding methods include hot compression molding, microinjection molding, laser direct-writing ablation, and *in situ* forming [2]. On the one hand, hot compression molding is a simple technology that has high molding accuracy [3], long cycle time, and low production efficiency. On the other hand, microinjection has high production efficiency. The mold process and construction of injection molding machine are complex, and the production cost using microinjection is high [4].

In recent years, numerous reports have been published about laser direct-writing ablation, which can be classified as either cold ablation or hot ablation. Cold ablation refers to laser generated photochemical degradation and ablation on the polymer matrix. An example of cold ablation is the excimer laser ablation of polymer microstructure [5]. For microstructures with a larger area, excimer laser ablation lasts longer and incurs greater cost. Hot ablation utilizes the thermal effect of laser to conduct thermal decomposition ablation. Mohammed *et al.* [6, 7] studied the microstructural channels of CO<sub>2</sub> laser direct-writing ablation poly(methyl methacrylate) (PMMA) substrate, with laser power between 10 and 60 W and scanning speed between 80 and 400 mm/s. They obtained a cross-section of microstructural channels from tens to hundreds of microns with high processing efficiency and low cost. In the hot ablation process, leaving the condensation material on the surface is easy. However, controlling the microstructural shape and dimension is difficult [8, 9]. *In situ* molding refers to the lithography (LIGA) method, which includes photoetching, electroforming, replication and other complex manufacturing processes. *In situ* molding of polymer microfluidic chip used the LIGA method [10, 11].

At present, the thermal effect of CO<sub>2</sub> laser and ablation microstructural channel are used, and studies on polymer material surface modification, cutting, and welding have been conducted [12–14]. However, few studies on PMC laser melting molding exist. In this study, based on previous experimental studies on CO<sub>2</sub> laser melting polymer [15], we developed a laser melting molding device, and CO<sub>2</sub> laser positioning irradiation method was adopted for a microstructural melting molding experiment using PMMA substrate. Through numerical analysis and experimental research, the factors influencing molding quality were analyzed and a new PMC laser melting molding method was used as reference.

## EXPERIMENTAL PART

### Materials and experimental devices

Poly(methyl methacrylate) (PMMA) with trade name TF001 was supplied by New Lake (China).

The sample was a round sheet 4000 μm in diameter and 1000 μm thick. The design of the part and microstruc-

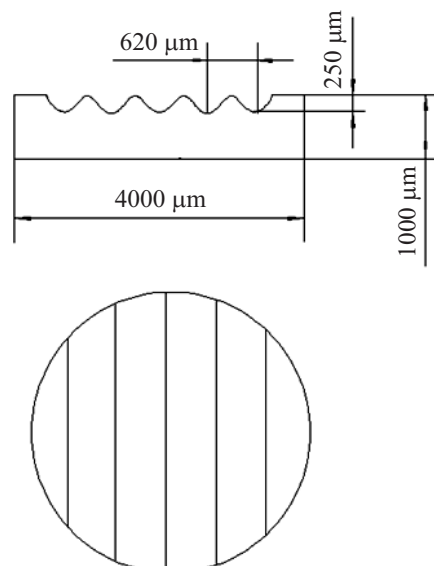


Fig. 1. Design charts of the part and microstructures

ture characteristics is presented in Fig. 1. The microstructure was designed as five continuous ripples. Each ripple was 620 μm wide and 250 μm high.

The experimental devices include both laser device and the mold, as shown in Fig. 2. The laser device used was a commercial laser machine (CLS2000, China) that could continuously generate a CO<sub>2</sub> laser beam, with the wavelength of 10.64 μm and power between 0 and 50 W. A laser beam with a diameter of from 0.15 to 20 mm was obtained by adjusting the lens. The mold was mainly formed by the restraint layer, template, mold core, the temperature controller, elevator and pressure controller. The restraint layer was formed by a ZnSe window glass. The ZnSe material showed a CO<sub>2</sub> laser transmittance rate of 99 %. The mold core was made of die steel, and electric sparks were used in the precise processing of microstructured features.

For testing the microstructured features of the mold core and molded part digital microscope system (VHX-1000, Japan) were used. Fig. 3 shows a photo and the microstructural three-dimensional shape of the mold core. The width (C-D) of the ripple measured as a cross-section of the middle ripple was 620.7 μm and its height was (A-B) 251.2 μm.

True-color confocal scanning microscope (Zeiss-Axio CSM 700, Germany) was used to measure the surface roughness of the mold and molded part.

## NUMERICAL SIMULATION

### Numerical model of laser melting specimen

In molding by laser melting, specimen temperature is the key to microstructure molding. The experiment used the basic mode of CO<sub>2</sub> laser, and the beam energy showed Gaussian distribution. The power density of light beams can be calculated using the following equation [16]:

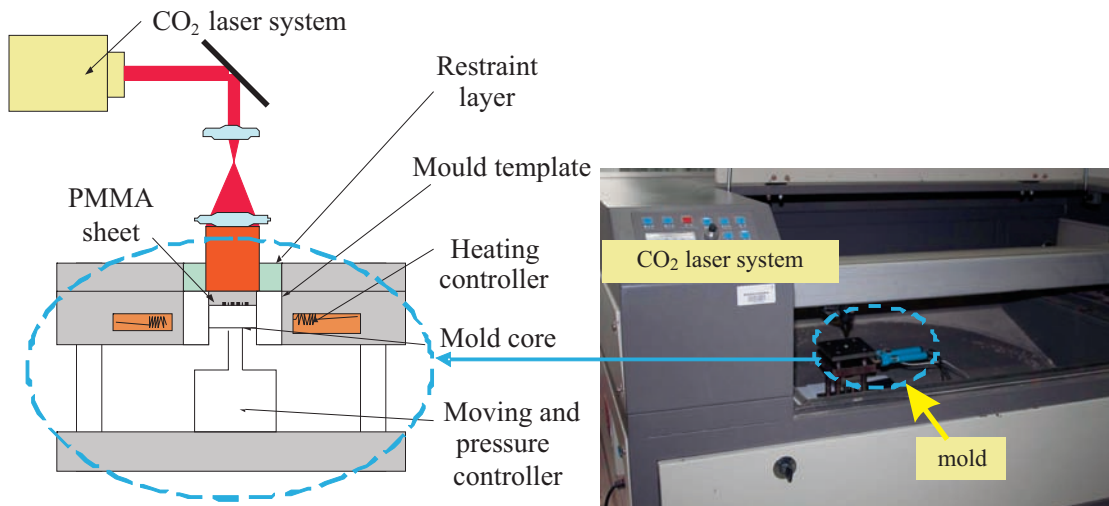


Fig. 2. Laser device and mold

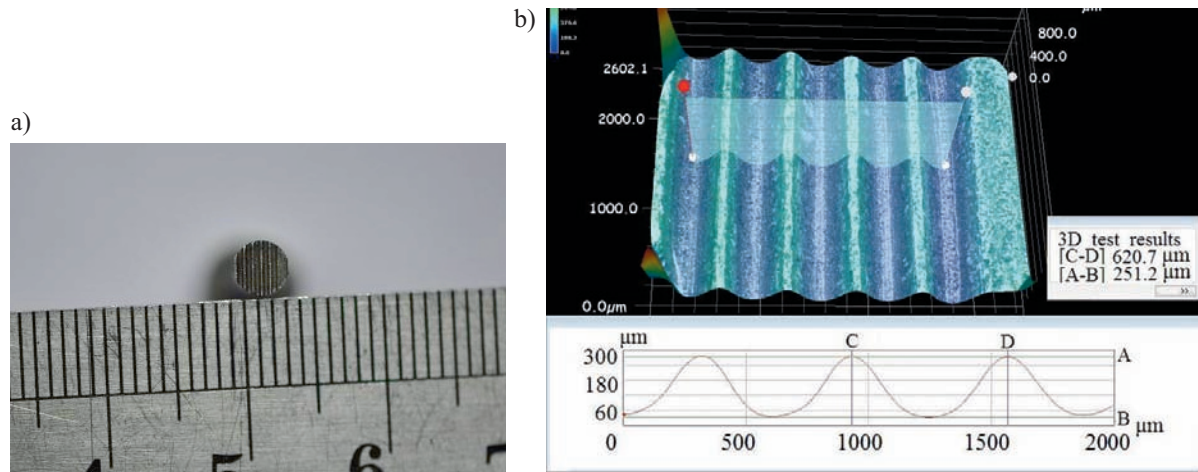


Fig. 3. Topography of mold core: a) photograph of mold core, b) cross-section profile of mold core

$$P_{(x,y)} = \frac{2P_0}{\pi r^2} \exp\left(-2\frac{x^2 + y^2}{r^2}\right) \quad (1)$$

where:  $P_0$  — the laser power,  $r$  — the radius of laser beam.

The material performance was assumed to be isotropic, and the beams were vertically radiated onto the specimen surface. The specimen surface absorbed the laser energy, and the heat transfer abided by the Fourier's law. The specimen temperature field  $[T_{(x, y, z, t)}]$  and the heat conduction equation in the area adjacent to the light spot at time  $t$  are as follows [16]:

$$T_{(x,y,z,t)} - T_0 = \frac{2P_0\sqrt{a}}{k\pi^{3/2}} \cdot \int_0^t \exp\left[-2\frac{x^2 + y^2}{8a(t-t')+r^2} - \frac{z^2}{4a(t-t')}\right] \cdot \frac{dt'}{\sqrt{t-t'}[8a(t-t')+r^2]} \quad (2)$$

$$\frac{\partial}{\partial x}\left(a\frac{\partial T}{\partial x}\right) + \frac{\partial}{\partial y}\left(a\frac{\partial T}{\partial y}\right) + \frac{\partial}{\partial z}\left(a\frac{\partial T}{\partial z}\right) + P_{(x,y)} = \frac{\partial}{\partial t}(c\rho T) \quad (3)$$

where:  $T_0$  — the ambient temperature,  $c$  — the thermal capacity,  $\rho$  — the material density,  $k$  — the thermal conductivity,  $a$  — the laser absorption coefficient.

Equations (1), (2) and (3), as well as the initial conditions ( $t = 0, T = T_0$ ) were considered to solve the temperature field distribution at  $t$ .

### Simulation software

The specimen temperature during the laser melting process was analyzed using finite element software Comsol V4.3. First, finite element modeling was established. Given that the sample diameter is smaller than the mold cavity, we believe that only the bottom of the sample made contact with the mold. The established model is composed of the sample and mold, as shown in Fig. 4a. The boundary conditions and loading conditions are set at 20 °C initial temperature, 1.0 W laser power, and 6 mm spot diameter. Each coefficient of the PMMA and steel mold is listed in Table 1.

Figs. 4b–4d show the temperature profiles of samples obtained for various time of laser irradiation. In the case of 3 s laser irradiation the sample temperature was between 85 and 193 °C, and this temperature was lower than the softening temperature. As the irradiation time

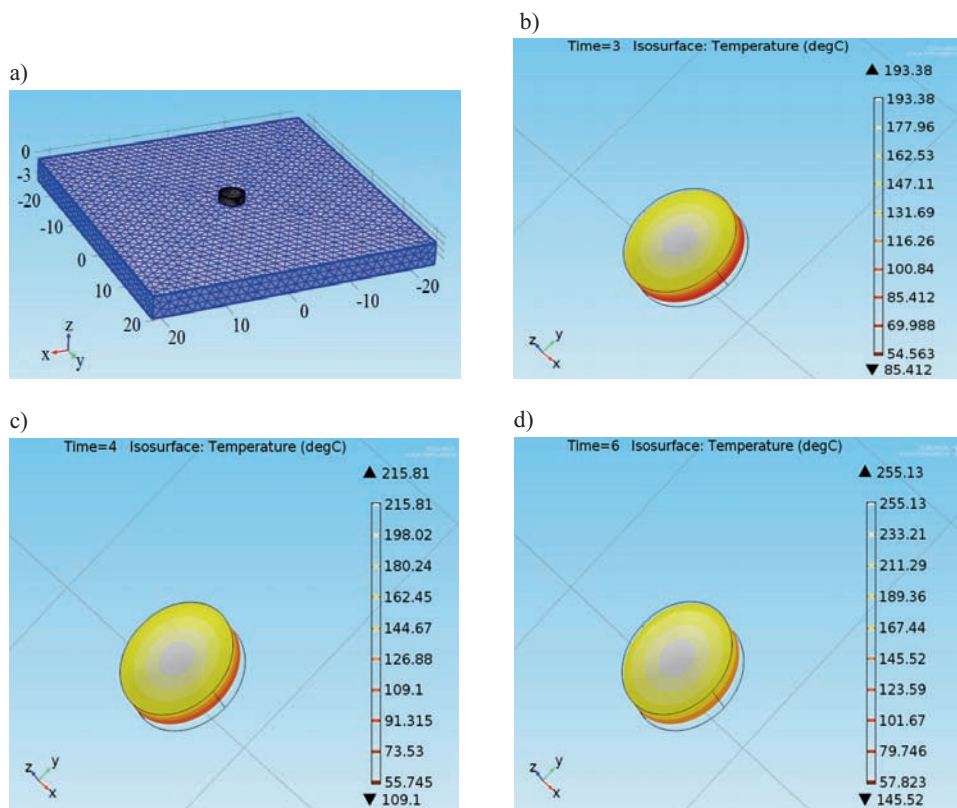


**Fig. 4.** Simulation of specimen temperature distribution: a) finite-element modeling, b) irradiation time 3 s, c) irradiation time 4 s, d) irradiation time 6 s

increased, the sample temperature improved. For 4 s laser irradiation the sample temperature was between 109 and 215 °C, which indicated that the entire sample had exceeded the glass transition temperature. The sample temperature for 6 s laser irradiation was between 145 and 255 °C, which indicated that the sample had melted completely. Fig. 5 summarizes the variation of the minimal and maximal sample temperatures depending on the duration of the laser irradiation.

**Table 1.** Parameters of PMMA and steel mold

	PMMA sample	Steel mold
Thermal conductivity, W/(m·K)	0.19	44.44
Thermal capacity, J/kg/K	1420	498
Density, kg/m <sup>3</sup>	1190	7850
Glass transition temperature ( $T_g$ ), °C	105	—
Flow temperature, °C	140	—
Degradation temperature, °C	270	—

## RESULTS AND DISCUSSION

### Experimental process

Initially the laser parameters were determined and the spot diameter was adjusted to 6 mm. When the power was 1.0 W and laser irradiation lasted for 4 s, the sample reached the softening state. The sample melted com-

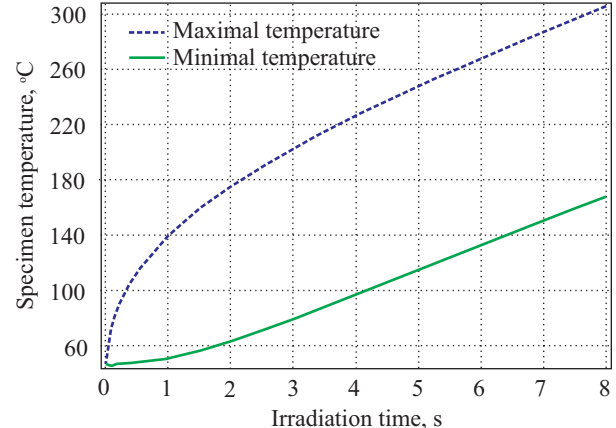


**Fig. 5.** Variation process of the specimen temperature

pletely after 6 s of laser irradiation. When laser irradiation lasted for more than 7 s, thermal decomposition and gasification occurred. The experimental results were consistent with the results of the numerical simulation. Therefore, in the melting molding process, the spot diameter was unchanged. The technological parameters, including laser power (0.8–1.2 W), irradiation time (3 to 6 s), molding force (50 to 200 N), and pressure retaining (30 s) were selected for repeated experiments. The molded part is shown in Fig. 6.

The microstructural three-dimensional shapes and cross-section dimensions of the parts obtained by molding with 4 s or 6 s laser irradiation (process parameters:

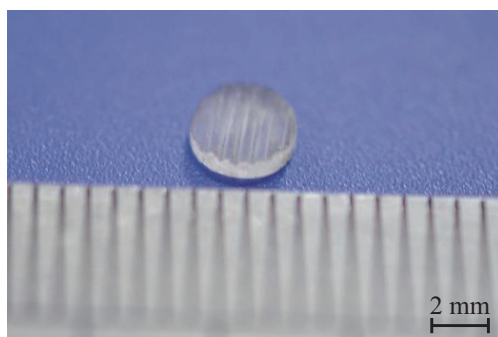


Fig. 6. Picture of the molded part

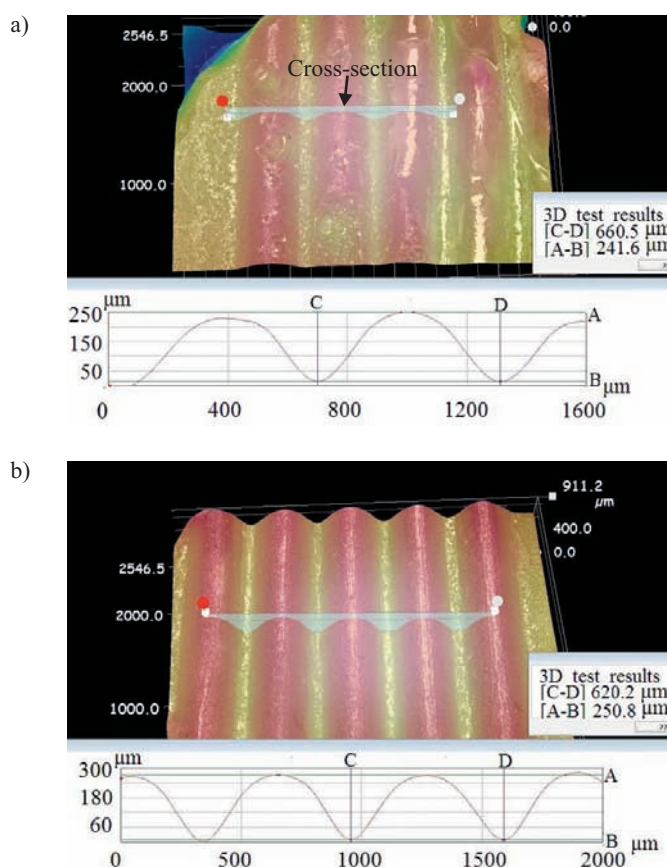


Fig. 7. Cross-section profiles of the molded parts obtained using irradiation time of: a) 4 s, b) 6 s

1.2 W laser power, 6 mm beam diameter, 80 °C mold temperature, and 100 N molding force) are shown Fig. 7. The middle ripples are 660.5  $\mu\text{m}$  wide and 241.6  $\mu\text{m}$  high (Fig. 7a) and 620.2  $\mu\text{m}$  wide and 250.8  $\mu\text{m}$  high (Fig. 7b) for parts irradiated for 4 or 6 s, respectively.

The microstructural shape of the mold was not complete because of the short irradiation time, as shown in Fig. 7a. In Fig. 7b, better microstructural molding quality is indicated for part with longer irradiation time. The dimension deviation of the middle ripple between parts shown in Fig. 3b and Fig. 7a were 39.6  $\mu\text{m}$  in width and 9.6  $\mu\text{m}$  in height, and the dimension deviation of the middle ripple between parts presented in Fig. 3b and Fig. 7b were 0.5  $\mu\text{m}$  in width and 0.4  $\mu\text{m}$  in height.

## Analysis of results

### Orthogonal experiment design

Considering the numerical simulation and experimental results, Minitab software was used to design the orthogonal experiment. Under the conditions of the set laser beam, the relatively feasible influencing factors adopted in this experiment included laser power, irradiation time, mold temperature, and molding pressure. For each factor, four levels were applied. The values of each mentioned factor for each level are listed in Table 2. To facilitate the analysis of the effects of processing parameters on the part quality, we defined the difference in microstructure height between the part and mold core as repetition accuracy.

Table 2. Experimental factors of the molding process corresponding to four levels

Level	Laser power, W	Irradiation time, s	Molding force, N	Mold temperature, °C
1	0.8	3	50	50
2	0.9	4	100	60
3	1.0	5	150	70
4	1.2	6	200	80

Table 3. Design and test results of the orthogonal experiment

Number	Laser power W	Irradiation time, s	Molding force N	Mold temperature °C	Dimensional deviation $\mu\text{m}$
1	0.8	3	50	50	250.0
2	0.8	4	100	60	192.5
3	0.8	5	150	70	83.7
4	0.8	6	200	80	29.2
5	0.9	3	100	70	250.0
6	0.9	4	50	80	105.6
7	0.9	5	200	50	52.5
8	0.9	6	150	60	16.7
9	1.0	3	150	80	250.0
10	1.0	4	200	70	93.2
11	1.0	5	50	60	28.6
12	1.0	6	100	50	6.2
13	1.2	3	200	60	196.0
14	1.2	4	150	50	46.3
15	1.2	5	100	80	3.5
16	1.2	6	50	70	0.3

The microstructured parts were longer along the ripple direction. The middle ripple was selected for the evaluation of height deviation. In this study, the arrangement of orthogonal experiment, recorded data and computational results are listed in Table 3. From Table 4, which presents the responding coefficients, laser power was the decisive factor that influenced the repetition

accuracy of the microstructure. The scanning time and mold temperature were secondary factors. The molding pressure had relatively lower influence than other factors.

**T a b l e 4.** Response table of data means

Level	Laser power, W	Scanning time, s	Molding force, N	Mold temperature, °C
1	1.981	1.998	1.712	1.811
2	1.732	1.751	1.635	1.792
3	1.643	1.711	1.773	1.754
Delta	0.460	0.259	0.067	0.196
Rank	1	2	4	3

Levels of the selected factors were correlated with indicators as required, and the deviation should be as small as possible. Through the combination of factors at better levels, optimal technological conditions can be achieved, namely, level 4 of laser power, level 4 of irradiation time, level 3 of molding pressure and level 4 of mold temperature. The optimal technological parameters combination is adjusted as follows: 1.2 W laser power, 6 s irradiation time, 150 N molding pressure, 80 °C mold temperature and 30 s pressure holding time.

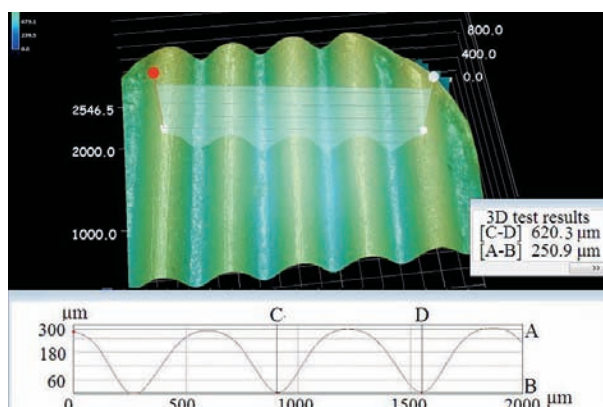


**Fig. 8.** Cross-section profile of the molded part using optimization parameters

The microstructure of the PMMA substrate obtained in the experiment with optimized parameters is presented in Fig. 8. This part shows better microstructure shape consistency between the molded piece and the mold in comparison to the part shown in Fig. 3b. The dimension deviations were 0.4 μm in width and 0.3 μm in height.

#### Surface quality

Surface roughness of the molded part is an evaluation standard of the molding quality. Using optimized technological parameters, we adopted molds of various surface roughness for the molding experiments.

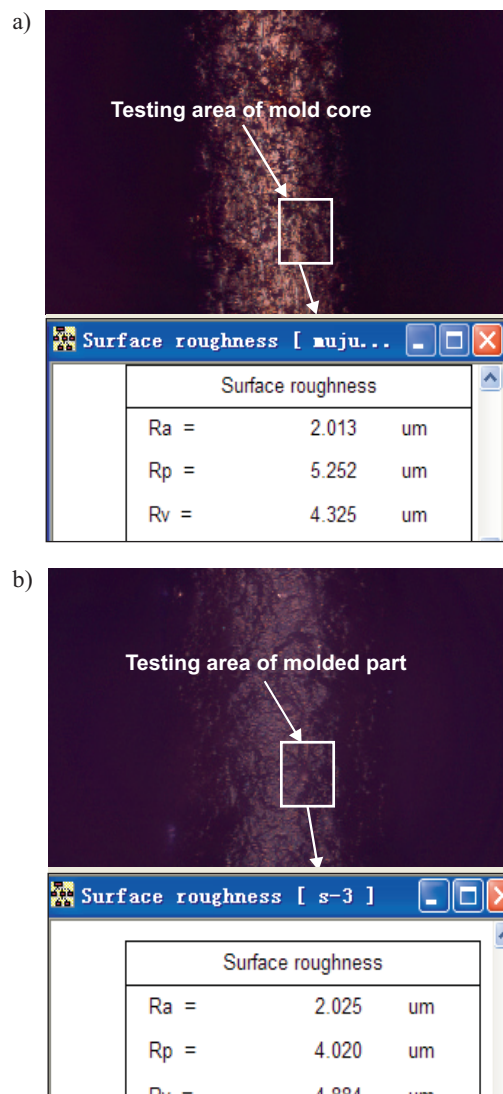


**Fig. 9.** Surface morphology and roughness of the mold core (a) and molded part (b)

The surface roughness was measured using true-color confocal scanning microscope. In the microstructural intermediate region of the mold and the molded part, the ripple bottom and surface were tested. The test results are shown in Fig. 9. The surface microtopography and roughness of the mold and the molded part are respectively presented.  $R_a$ ,  $R_p$  and  $R_v$  represent the arithmetic mean variation of the superficial outline, mean peak height and mean valley depth of the outline, respectively.

**T a b l e 5.** Roughness of molds and molded parts

Group number	Mold core $R_a$ μm	Molded part $R_a$ μm	Difference μm
1	2.013	2.025	0.012
2	3.446	3.804	0.358
3	5.975	8.432	2.457
4	6.261	9.793	3.532
5	8.053	16.579	8.526

As shown in Fig. 9 the roughness differences were for  $R_a$  0.012  $\mu\text{m}$ , for  $R_p$  1.23  $\mu\text{m}$ , and for  $R_v$  0.56  $\mu\text{m}$ .  $R_a$  can relatively represent the characteristics of the superficial outline. Thus,  $R_a$  is employed for analysis. The results for five groups with different mold roughness and molded parts are listed in Table 5. The mold with higher surface accuracy allows obtaining the molded part with lower surface roughness.

## CONCLUSION

This paper proposed the use of PMC laser melting molding method, which refers to a low-power CO<sub>2</sub> laser irradiation in which the polymer melts in the mold and extrudes into the molding. Numerical simulation and experimental results demonstrated that the melting temperature is a key factor influencing the molding quality. By optimizing technological parameters, we obtained relatively higher microstructural replication accuracy. The consistency between the molded piece and the mold was found. In addition, the mold with lower surface roughness can be used to obtain the molded piece with higher surface accuracy, and with extremely small difference of  $R_a$ .

*This work was financially supported by National Nature Science Foundation of China (No. 51175236), Jiangsu Province “333 Project” funded project and the Changzhou, Jiangsu Science and Technology Project (No. CJ20140003).*

## REFERENCES

- [1] Mohammed M.I., Desmulliez M.P.Y.: *Lab. Chip.* **2011**, *11*, 569. <http://dx.doi.org/10.1039/C0LC00204F>
- [2] Becker H., Gärtner C.: *Anal. Bioanal. Chem.* **2008**, *390*, 89. <http://dx.doi.org/10.1007/s00216-007-1692-2>
- [3] Becker H., Heim U.: *Sens. Actuators A: Phys.* **2000**, *83*, 130.
- [4] Giboz J., Copponnex T., Mélé P.: *J. Micromech. Microeng.* **2007**, *17*, R96. <http://dx.doi.org/10.1088/0960-1317/17/6/R02>
- [5] Costela A., Garciamoreno I., Florido F.: *J. Appl. Phys.* **1995**, *77*, 2343. <http://dx.doi.org/10.1063/1.358756>
- [6] Mohammed M.I., Abraham E.M., Desmulliez P.Y.: *J. Micromech. Microeng.* **2013**, *23*, 035034. <http://dx.doi.org/10.1088/0960-1317/23/3/035034>
- [7] Qi H., Wang X.S., Chen T. et al.: *J. Chinese Lasers* **2009**, *36*, 1239.
- [8] Li J.M., Liu C., Zhu L.Y.: *J. Mater. Process Tech.* **2009**, *209*, 4814. <http://dx.doi.org/10.1016/j.jmatprotec.2009.01.001>
- [9] Zhang Z., Wang X., Luo Y., Wang L.: *J. Thermoplast. Compos. Mater.* **2009**, *23*, 647. <http://dx.doi.org/10.1177/0892705709356493>
- [10] Kim J., Xu X.: *J. Laser Appl.* **2003**, *15*, 255.
- [11] Xu S.J., Duan Y.G., Ding Y.C., Lu B.H.: *J. China Mech. Eng.* **2007**, *43*, 105.
- [12] Romoli L., Tantussi G., Dini G.: *Opt. Laser. Eng.* **2011**, *49*, 419. <http://dx.doi.org/10.1016/j.optlaseng.2010.11.013>
- [13] Waugh D.G., Lawrence J.: *Opt. Laser. Eng.* **2010**, *48*, 707. <http://dx.doi.org/10.1016/j.optlaseng.2010.01.005>
- [14] Huang Y.G., Liu S.B., Yang W., Yu C.X.: *Appl. Surf. Sci.* **2010**, *256*, 1675. <http://dx.doi.org/10.1016/j.apsusc.2009.09.092>
- [15] Tan W.S., Zhou J.Z., Huang S.: *Adv. Mater. Res.* **2012**, *472*, 2514.
- [16] Li J.C.: “The calculation of laser diffraction and thermal acting”, Beijing Science publisher, Beijing 2008, p. 344.

Received 27 V 2014.